

## The $\nabla \cdot \mathbf{B} = 0$ Constraint in Shock-Capturing Magnetohydrodynamics Codes

Gábor Tóth

*Dept. of Atomic Physics, Eötvös Univ., Pázmány sétány 1, 1117 Budapest, Hungary  
Space Research Lab, Univ. of Michigan, 2455 Hayward, Ann Arbor MI 48109, USA*

This proceedings is a brief summary of a rather long paper with the same title and author, which is expected to appear in part 2 of volume 161 of the Journal of Computational Physics in July 2000. Please see the published paper for more details and references.

There has been a very rapid development towards shock-capturing numerical methods applied to the equations of magnetohydrodynamics (MHD). Still, there are unresolved arguments about how one should maintain the divergence free property of the magnetic field in multidimensional MHD calculations. Ideally, one would like to have that *particular* representation to be zero, which ensures that no unphysical effects arise, for example the plasma should not be accelerated parallel to the field lines by the discretized Lorentz force. It can be proved, however, that a scheme cannot satisfy both the numerical conservation of momentum (which is necessary to obtain correct jump conditions across a shock) and the requirement that the discretized acceleration due to the Lorentz force should be exactly perpendicular to the magnetic field in every grid cell. The schemes discussed below use various simple discretizations of  $\nabla \cdot \mathbf{B}$ , but clearly the choice is always somewhat arbitrary and only numerical tests can tell which scheme is the most efficient, accurate, and robust for a particular class of problems.

In the context of shock-capturing MHD codes, three approaches became rather popular to handle the  $\nabla \cdot \mathbf{B} = 0$  constraint: the 8-wave scheme, various constrained transport type schemes, and the projection scheme. All three approaches can be regarded as some modification of, or addition to a shock capturing base scheme.

**The base scheme** can be any shock capturing method. In the numerical tests below the base scheme is the dimensionally split Total Variation Diminishing (TVD) scheme by Harten or, when the TVD base scheme fails, the dimensionally unsplit TVD-MUSCL scheme by van Leer with a Hancock predictor step. In both base schemes the sharp monotized central (MC) limiter or, when that fails, the more diffusive but more robust minmod limiter is used. The base scheme evolves  $\rho$ ,  $\rho\mathbf{v}$ ,  $e$ , and  $\mathbf{B}$  (the mass, momentum, and energy densities, and the magnetic field, respectively), but it is modified in some way to maintain the  $\nabla \cdot \mathbf{B} = 0$  constraint. All these algorithms are implemented in the Versatile Advection Code (see <http://www.phys.uu.nl/~toth/>).

**The 8-wave scheme** was introduced by Powell. This scheme allows the numerical value of  $\nabla \cdot \mathbf{B}$  to become non-zero, but it discretizes a rederived form of the MHD equations in which the  $\nabla \cdot \mathbf{B} = 0$  Maxwell equation has not been used:

$$\frac{\partial \rho}{\partial t} + \nabla \cdot (\rho\mathbf{v}) = 0 \quad (1)$$

$$\frac{\partial \rho\mathbf{v}}{\partial t} + \nabla \cdot (\mathbf{v}\rho\mathbf{v} - \mathbf{B}\mathbf{B}) + \nabla(p + \frac{1}{2}\mathbf{B}^2) = -(\nabla \cdot \mathbf{B})\mathbf{B} \quad (2)$$

$$\frac{\partial e}{\partial t} + \nabla \cdot [\mathbf{v}(e + p + \frac{1}{2}\mathbf{B}^2) - \mathbf{B}\mathbf{B} \cdot \mathbf{v} - \mathbf{B} \times \eta\mathbf{J}] = -(\nabla \cdot \mathbf{B})\mathbf{B} \cdot \mathbf{v} \quad (3)$$

$$\frac{\partial \mathbf{B}}{\partial t} + \nabla \cdot (\mathbf{v}\mathbf{B} - \mathbf{B}\mathbf{v}) + \nabla \times (\eta\mathbf{J}) = -(\nabla \cdot \mathbf{B})\mathbf{v} \quad (4)$$

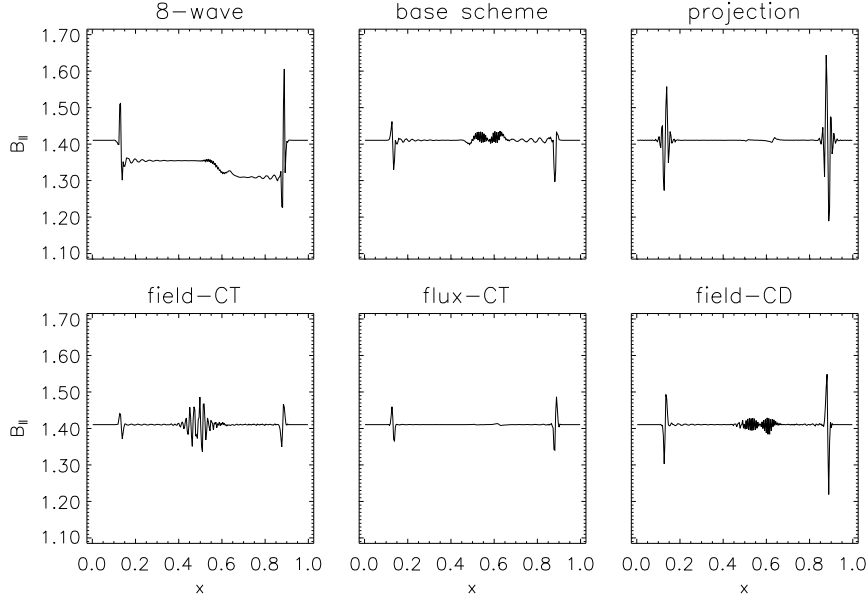


Figure 1: The parallel component of the magnetic field in a 2D rotated shock tube test is shown for six different schemes.

where  $p = (\gamma - 1)(e - \rho\mathbf{v}^2/2 - \mathbf{B}^2/2)$  is the thermal pressure with the adiabatic index  $\gamma$ ,  $\eta$  is the resistivity,  $\mathbf{J} = \nabla \times \mathbf{B}$  is the current, and units of  $\mathbf{B}$  are such that the vacuum permeability is unity. The only new terms relative to the usual form are the right hand side source terms proportional to  $\nabla \cdot \mathbf{B}$ . The 8-wave scheme is the discretization of the above system of equations. The inclusion of the non-conservative source terms usually improve robustness and accuracy, however, according to the Lax-Wendroff theorem only conservative schemes are guaranteed to get the correct jump conditions and propagation speed for a discontinuous solution. In one of the numerical tests the 8-wave scheme was indeed found to produce an erroneous value for the the magnetic field component parallel with the shock normal as shown in Fig. 1. This error does not reduce with resolution. In the other variables of this test, and in all variables of all the other 9 tests, however, no significant error has been found which could be related to incorrect jump conditions.

**The constrained transport (CT)** schemes (introduced by Evans and Hawley) use simple finite difference formulae to solve the induction equation which conserve  $\nabla \cdot \mathbf{B}$  in a specific discretization. If the initial magnetic field has zero divergence in this discretization, then every time step will maintain that to the accuracy of machine round off error as long as the boundary conditions are compatible with the constraints. In their original formulation the CT type schemes require a staggered discretization of the magnetic field components as shown in the left panel of Fig. 2. The electric field is approximated at the cell corners either by interpolating  $\mathbf{v}$  and  $\mathbf{B}$  from the surrounding cells (**field-CT scheme**) or by interpolating upwind fluxes of the base scheme from the surrounding cell faces (**flux-CT scheme**). The electric field is finite differenced to evolve the face centered magnetic field components as

$$\begin{aligned} B_{j+1/2,k}^{x,n+1} &= B_{j+1/2,k}^{x,n} - \Delta t \frac{E_{j+1/2,k+1/2}^z - E_{j+1/2,k-1/2}^z}{\Delta y} \\ B_{j,k+1/2}^{y,n+1} &= B_{j,k+1/2}^{y,n} + \Delta t \frac{E_{j+1/2,k+1/2}^z - E_{j-1/2,k+1/2}^z}{\Delta x} \end{aligned} \quad (5)$$

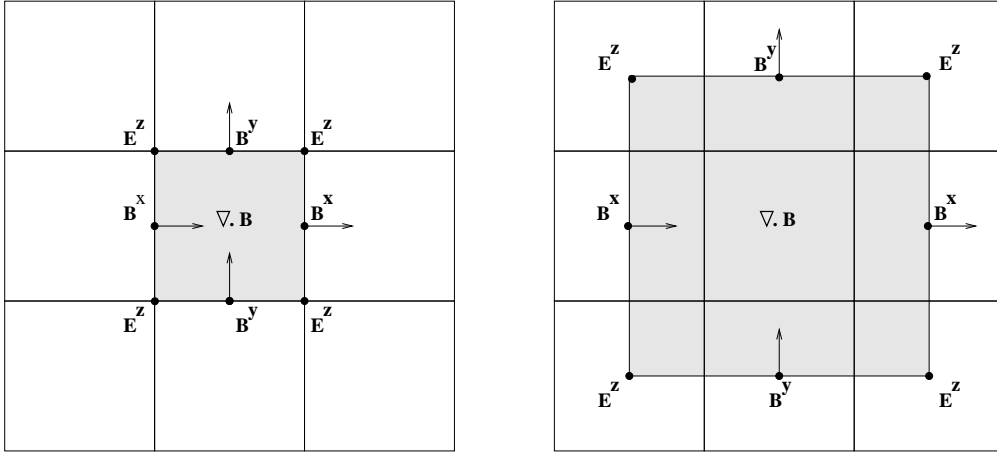


Figure 2: The staggered (left) and cell centered (right) discretizations of the CT and CD schemes, respectively.

The staggered field components are then interpolated to cell centers to be used by the base scheme. It can be shown, however, that the staggered variables can be eliminated from both CT algorithms, and they can be cast into pure finite volume schemes.

**The new and simple central difference (CD)** approach uses cell centered discretization for all variables as shown in the right panel of Fig. 2. The magnetic field components are updated as

$$\begin{aligned} B_{j,k}^{x,n+1} &= B_{j,k}^{x,n} - \Delta t \frac{E_{j,k+1}^z - E_{j,k-1}^z}{2\Delta y} \\ B_{j,k}^{y,n+1} &= B_{j,k}^{y,n} + \Delta t \frac{E_{j+1,k}^z - E_{j-1,k}^z}{2\Delta x} \end{aligned} \quad (6)$$

where the cell centered electric field can be either obtained by temporal interpolation of the local base scheme electric field (**field-CD scheme**), or by spatial interpolation of base scheme fluxes through the surrounding cell faces (**flux-CD scheme**). All four CT/CD schemes can be generalized to 3D, to axial symmetric calculations, and to arbitrary curvilinear grids.

**The projection scheme**, in the context of MHD, was suggested by Brackbill and Barnes. The idea is to project the numerical solution  $\mathbf{B}^* = \nabla \times \mathbf{A} + \nabla\phi$  provided by the base scheme onto the subspace of zero divergence solutions. First the Poisson equation

$$\nabla^2 \phi = \nabla \cdot \mathbf{B}^* \quad (7)$$

is solved and then the magnetic field is corrected to

$$\mathbf{B}^{n+1} = \mathbf{B}^* - \nabla\phi \quad (8)$$

It can be shown that the projected  $\mathbf{B}^{n+1}$  is the closest divergence free field to  $\mathbf{B}^*$ . It has been questioned in the literature whether the projection scheme is valid for discontinuous flows. I proved that the projection scheme is consistent and it has the same order of accuracy as the base scheme for continuous and discontinuous problems as well. Another concern for the projection scheme is the efficiency and flexibility of the Poisson solver. Using a limited number of conjugate gradient type iterations, the Poisson problem can

Table 1: Numerical errors relative to the most accurate scheme for each test

	project.	field-CD	flux-CT	flux-CD	8-wave	field-CT	base
Alfvén travelling	1.000	2.177	2.491	2.491	1.005	3.562	1.002
Alfvén standing	1.000	1.374	1.219	1.219	1.599	1.339	1.168
2D shock $\alpha=63^\circ$	1.022	1.005	1.000	1.007	1.268	1.269	1.006
2D shock $\alpha=45^\circ$	1.000	1.031	1.047	1.047	1.801	1.298	1.782
2.5D shock tube	1.000	1.137	1.234	1.234	1.023	1.392	1.333
Orszag $t=1$	1.259	1.000	1.324	1.415	1.425	1.127	1.498
Orszag $t=3.14$	1.132	1.000	1.188	1.233	1.411	1.187	1.893 <sup>a</sup>
Cloud-shock	1.007	1.069	1.000	1.036	1.013	1.072	1.348 <sup>a</sup>
Rotor $p=1$	1.000	1.220	1.052	1.216	1.023	1.530	1.094
Rotor $p=0.5$	1.000	1.058	1.098	1.116	1.050	1.289	1.071
Correction factor	$\approx 1.06$	1.006	1.018	1.013	1.023	1.014	1.000

<sup>a</sup> Required use of the minmod limiter at some resolution(s)

be solved with sufficient accuracy while the computational cost increases only by about 20 – 30% relative to the base scheme. These iterative schemes work in any geometry, with a large variety of boundary conditions, and they also easily parallelize.

**10 numerical tests** are done with 7 schemes at 2 or 3 different grid resolutions. The quantitative errors are measured with respect to an analytic or a high resolution numerical solution. The relative errors, normalized in each variable, are averaged for all the primitive variables. These average relative errors are compared for all the schemes, and normalized to the scheme with the smallest error. Finally, the normalized average relative errors are further averaged for all the examined grid resolutions, and reported in Table 1 for the 10 test problems. The last row of the table contains a correction factor which is the cubic root of the computational cost of the scheme relative to the base scheme.

The first 5 tests are physically 1D problems, but they are rotated by  $\alpha$  in the 2D  $x - y$  plane. In the 1st and 2nd tests circularly polarized travelling and standing Alfvén waves are simulated, respectively. These smooth flows with known analytic solutions test the order of accuracy as well as amplitude and phase errors. Although all schemes converge at a second order rate as expected, at coarse resolution there are quite significant differences in accuracy (see top 2 lines of Table 1). The 3rd to 5th tests are rotated shock tube problems. The rest of the tests are true 2D problems: the Orszag-Tang vortex at two different times, the interaction of a fast shock with a dense cloud, and a magnetized rotor problem with 2 different values for pressure.

**Based on the examined test problems the projection, the new field-CD, and the flux-CT schemes are found to be the most accurate and reliable.** It would be interesting to see how well the different schemes can solve steady state problems, how they can be combined with implicit time integration, or how they can be adapted to hierarchical or adaptively refined meshes, however, these questions are out of the scope of this paper and subject of future research.

**Acknowledgements:** The development of the Versatile Advection Code was funded by the Dutch Science Foundation (NWO) from 1994 to 1997. This research was mainly supported by a postdoctoral fellowship (D 25519) from the Hungarian Science Foundation (OTKA) and by the Bolyai Fellowship from the Hungarian Academy of Sciences. Final improvements were done while working at the University of Michigan as a research scientist.